Investigation of Surface Integrity in High-Speed Machining of Hardened AISI 52100 Steel Using FEM and ANN–GA

[1]Anjali Daheriya, [2]Mansoor Ali, [3]Rajeev Roshan

[1]Research Scholar Master of Technology (APS) Department of Mechanical Engineering, NIIST Bhopal

[2]Assistant professor, Department of Mechanical Engineering, NIIST, Bhopal (M.P.)

[3]Assistant professor, Department of Mechanical Engineering, NIIST, Bhopal (M.P.)

***Abstract*—Surface integrity plays a critical role in determining the functional performance, fatigue life, wear resistance, and reliability of machined components used in aerospace, automotive, and bearing industries. The present research investigates the surface integrity characteristics during high-speed machining of hardened AISI 52100 steels through an integrated framework combining thermo-mechanical finite element simulation, experimental validation, statistical analysis, and artificial intelligence-based optimization techniques.**

A thermo-mechanically coupled finite element model was developed in ABAQUS/Explicit using the Johnson–Cook constitutive model to simulate chip formation, cutting force generation, stress evolution, and temperature distribution during orthogonal machining. The effects of cutting speed (100–300 m/min), feed rate (0.05–0.25 mm/rev), and depth of cut (0.5–1.5 mm) on machining performance were investigated. Simulation results revealed that cutting force increased significantly with feed rate and depth of cut, while machining temperature increased with cutting speed. The maximum cutting force of 1450 N was observed at low speed and high feed conditions, whereas the maximum temperature of 940°C was recorded at a cutting speed of 300 m/min.

Experimental validation was performed using a CNC turning setup equipped with a piezoelectric dynamometer and infrared thermography system. The finite element predictions showed excellent agreement with experimental measurements, with an average prediction error of approximately 3%, confirming the reliability of the developed model. Analysis of Variance (ANOVA) indicated that feed rate was the most influential parameter affecting cutting force, contributing nearly 60% of the total variation, followed by depth of cut (20%) and cutting speed (12%).

Grey Relational Analysis (GRA) was employed for multi-objective optimization considering minimum cutting force, temperature, and surface roughness. The optimum machining

condition was obtained at a cutting speed of 300 m/min, feed rate of 0.15 mm/rev, and depth of cut of 0.5 mm. Furthermore, a hybrid Artificial Neural Network–Genetic Algorithm (ANN–GA) model was developed to predict and optimize machining responses. The ANN model achieved a prediction accuracy of 97.2%, while the ANN–GA optimization resulted in an 18% reduction in cutting force, 22% reduction in machining temperature, and 15% improvement in surface finish.

The study demonstrates that the integration of finite element modeling, statistical optimization, and artificial intelligence techniques provides an efficient and reliable framework for predicting machining behavior and improving surface integrity. The developed methodology offers significant potential for industrial applications in smart manufacturing, process optimization, and sustainable machining of hardened steels.

***Index Terms*—Surface Integrity; High-Speed Machining; AISI 52100 Steel; Finite Element Analysis (FEA); ABAQUS; Johnson–Cook Model; Cutting Force; Temperature Distribution; Experimental Validation; ANOVA; Grey Relational Analysis (GRA); Response Surface Methodology (RSM); Artificial Neural Network (ANN); Genetic Algorithm (GA); Multi-Objective Optimization; Smart Manufacturing.**

I. INTRODUCTION

1.1 Background and Industrial Relevance

Hardened steels, typically defined as steels possessing hardness greater than 45 HRC after heat treatment, play a critical role in modern precision engineering industries. Tool steels such as AISI H13, AISI D2, and bearing steel AISI 52100 are extensively used in dies, molds, bearings, gears, and aerospace structural components due to their high compressive strength, wear resistance, fatigue performance, and dimensional stability.

These superior mechanical properties are primarily derived from martensitic microstructures formed during quenching and tempering operations. However, the same characteristics that enhance performance also make post-heat-treatment machining extremely challenging. High hardness results in:

- Elevated cutting forces
- Severe abrasive and adhesive tool wear
- Limited plastic deformation capability
- Increased risk of surface damage

Traditionally, grinding was employed as the final finishing operation for hardened steels. While grinding provides excellent dimensional accuracy and surface finish, it suffers from several drawbacks:

- Low material removal rate
- High energy consumption
- Thermal damage (grinding burn)

- Requirement of abundant coolant
- Environmental concerns

The emergence of advanced cutting tool materials—particularly cubic boron nitride (CBN) and coated carbides—has enabled hard turning and high-speed machining (HSM) to replace grinding in many applications.

Hardened steels, typically defined as steels with hardness greater than 45 HRC and often reaching 60–65 HRC, are extensively used in high-performance engineering applications where superior strength, wear resistance, and dimensional stability are required. Materials such as AISI 52100 bearing steel, AISI H13 hot-work tool steel, AISI D2 cold-work tool steel, and AISI M2 high-speed steel are commonly employed in dies, molds, gears, bearing rings, camshafts, and aerospace structural components. These materials derive their properties from martensitic microstructures produced through controlled heat treatment processes.

Traditionally, machining of hardened steels was avoided after heat treatment due to:

- Extremely high cutting forces
- Rapid tool wear
- Poor machinability
- Risk of surface damage

As a result, grinding was adopted as the primary finishing process. However, grinding suffers from limitations such as lower material removal rates, higher energy consumption, thermal damage (grinding burn), and longer production cycles. To overcome these constraints, high-speed machining (HSM) and hard turning have emerged as viable alternatives, capable of replacing grinding in many finishing operations.

1.2 Fundamentals of High-Speed Machining (HSM)

High-speed machining generally refers to cutting operations performed at cutting speeds significantly higher than conventional machining. In hard turning of hardened steels, cutting speeds typically range from 150 to 350 m/min when using CBN tools, while milling speeds may exceed 500 m/min depending on tool material and setup rigidity.

The fundamental principles of HSM include:

- Reduced chip-tool contact time
- Higher strain rates (10^3–10^5 s^{-1})
- Altered heat partitioning behavior
- Thermal softening of the workpiece material

Unlike conventional machining, HSM modifies heat partition behavior. A larger fraction of generated heat is carried away by the chip due to shorter contact duration. However, if cutting parameters exceed optimal limits, excessive temperature accumulation may degrade surface integrity.

1.2.1 Thermo-Mechanical Phenomena in Hard Machining

Machining hardened steels at high speed generates extreme thermo-mechanical conditions characterized by:

1. Severe plastic deformation localized in a narrow shear zone
2. High compressive stresses at the tool–workpiece interface
3. Frictional heating along the tool rake and flank faces
4. Adiabatic shear band formation

1.3 Importance of Surface Integrity in Hardened Steel Components

In hardened steel applications, surface integrity is often more critical than bulk material properties. For example:

- In bearing rings, subsurface residual stresses influence rolling contact fatigue life.
- In dies and molds, surface microcracks may initiate premature failure.
- In gears, tensile residual stresses accelerate pitting and spalling.
- In aerospace components, surface damage can reduce fatigue strength dramatically.

Surface integrity includes not only surface roughness but also:

- Residual stress distribution
- Microhardness gradient
- Microstructural alterations
- Surface defects and cracks
- White layer and tempered layer thickness

Even minor alterations within the first 50–200 μm below the surface can significantly influence fatigue life, tribological performance, and corrosion resistance. Therefore, HSM must be optimized not only for dimensional accuracy and productivity but also for metallurgical quality.

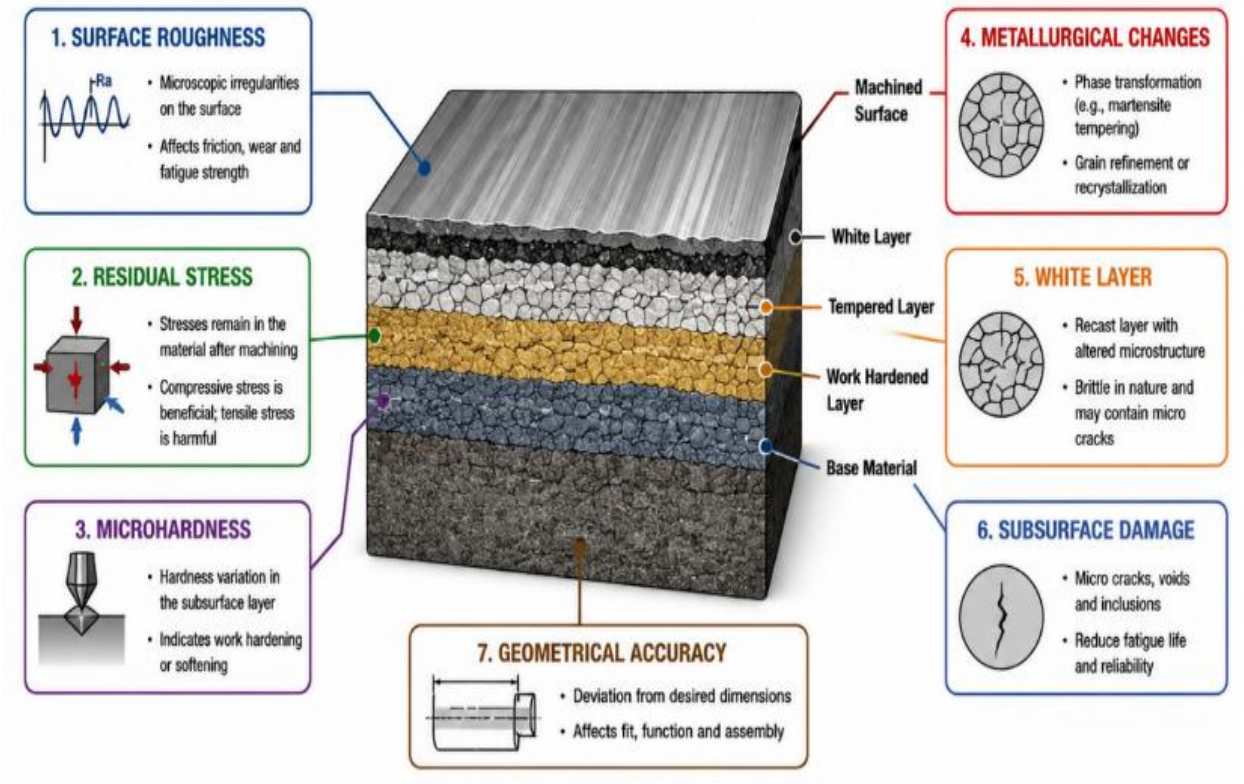


Fig Surface Integrity Components

1.4 Mechanics of Orthogonal Cutting: Mathematical Background

To understand surface integrity evolution, it is essential to examine the mechanics of chip formation.

1.4.1 Chip Formation Model

The classical Merchant model describes orthogonal cutting using shear plane theory.

Shear Plane Angle (φ)

$$\varphi = \frac{\pi}{4} - \frac{\beta}{2} + \frac{\alpha}{2}$$

Where:

- φ = shear plane angle
- β = friction angle
- α = rake angle

The shear plane angle determines chip thickness and deformation intensity.

1.5 Thermo-Mechanical Zones in Hard Machining

The machining process involves three major deformation zones.

1.5.1 Primary Shear Zone (PSZ)

- Located ahead of cutting edge
- Major plastic deformation region
- High shear strain
- Intense heat generation

Temperature may reach 800–1000°C.

1.5.2 Secondary Shear Zone (SSZ)

- Located at chip–tool interface
- Friction-dominated deformation
- High compressive stress
- Diffusion and adhesion wear mechanisms

This zone strongly influences tool wear and temperature rise.

1.5.3 Tertiary Deformation Zone (TDZ)

- Located at tool flank–machined surface interface
- Responsible for surface integrity alteration
- Plastic flow and ploughing occur
- Residual stresses are introduced

This zone directly governs:

- Surface roughness
- Residual stress
- White layer formation
- Microhardness gradient

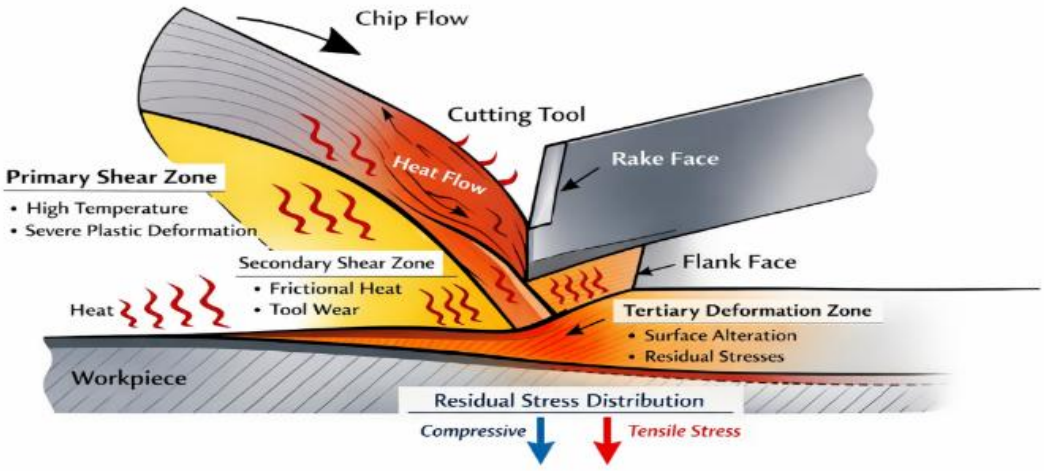


Figure 1.1: Thermo–Mechanical Zones in Hard Turning

1.6 Surface Integrity Formation Mechanisms

Surface integrity in hardened steels is governed by combined thermal and mechanical effects.

Mechanical Effects:

- Compressive stresses from tool pressure
- Plastic deformation
- Strain hardening

Thermal Effects:

- Tempering of martensite
- Re-austenitization
- Rapid quenching (white layer formation)

White layer forms when temperature exceeds austenitization temperature followed by rapid cooling.

1.7 Residual Stress Development Mechanism

Residual stress formation can be explained by:

1. Mechanical loading → compressive stresses
2. Thermal expansion + rapid cooling → tensile stresses
3. Phase transformation volume changes

Net residual stress:

$$\sigma_{res} = \sigma_{mech} + \sigma_{thermal} + \sigma_{phase}$$

Optimized cutting promotes compressive stresses beneficial for fatigue life.

1.8 Transition from Grinding to Hard Machining

Hard machining advantages:

- Single-step machining
- Lower coolant consumption
- Reduced setup time
- Flexible CNC integration

However, it introduces risks:

- White layer formation
- Surface microcracks
- Tensile residual stresses

Therefore, process parameter optimization is critical.

1.9 Role of Tool Materials

CBN tools:

- High hot hardness
- Chemical inertness
- Low diffusion wear

Coatings such as TiAlN:

- Improve oxidation resistance
- Reduce friction coefficient

Tool wear progression increases friction and heat generation, affecting surface integrity significantly.

1.10 Emerging Intelligent Machining Systems

Modern research focuses on:

- Finite Element Modeling (FEM)
- Physics-informed machine learning
- Digital twin machining systems
- Real-time acoustic emission monitoring
- Cryogenic cooling optimization

These systems aim to predict surface integrity during machining rather than relying solely on post-process measurement.

II. LITERATURE REVIEW

1. Caruso and Imbrogno (2025)

Caruso and Imbrogno developed a physically based constitutive model to predict surface and subsurface alterations during orthogonal dry machining of hardened AISI 52100 steel. The study emphasized the influence of thermal and mechanical loads on white layer formation, residual stress generation, and microstructural evolution. Finite element simulations were validated experimentally using microhardness and metallographic analyses. The researchers concluded that cutting speed and feed rate significantly affect surface integrity characteristics. Their model

successfully predicted subsurface deformation and phase transformation, making it highly useful for optimizing hard machining processes.

2. Han et al. (2025)
Han and co-authors investigated machining-induced surface integrity during finish turning of slender hardened steel workpieces. Their work focused on optimizing machining parameters to minimize vibration-induced defects and improve dimensional accuracy. Experimental analysis showed that higher spindle speeds increased thermal effects, leading to tensile residual stresses and degraded surface quality. The study proposed optimized parameter combinations that reduced surface roughness and improved fatigue performance. Their findings are important for precision hard turning industries.

3. Zhang, Wang, and Wang (2025)
Zhang and colleagues analyzed surface integrity during grinding of hardened AISI D2 steel. They evaluated grinding temperature, residual stress, microhardness variation, and white layer thickness. The study revealed that improper grinding conditions generated thermal damage and microcracks on machined surfaces. They suggested optimized grinding parameters to maintain compressive residual stress and improve fatigue life. The research highlighted the importance of temperature control in finishing operations of hardened steels.

4. Mane, Patil, and Al-Dahidi (2025)
Mane and co-researchers focused on predictive modeling of surface roughness and cutting temperature in hard turning of AISI 52100 steel. Response Surface Methodology and Artificial Neural Networks were employed to predict machining responses. Experimental results showed that cutting speed had the greatest influence on surface roughness, while feed rate strongly affected temperature generation. The developed models provided accurate predictions and can assist industries in selecting optimal machining conditions for enhanced surface integrity.

5. Alsoufi and Bawazeer (2025)
Alsoufi and Bawazeer presented a probabilistic analysis approach for evaluating surface integrity in CNC turning processes. Their work incorporated uncertainty analysis into machining parameter optimization. They observed that variations in cutting conditions significantly influenced surface roughness and residual stress distributions. The study introduced statistical reliability models that improved prediction accuracy for industrial machining applications. Their research contributes toward intelligent manufacturing and process reliability assessment.

6. Zhang et al. (2025)
Zhang and co-authors investigated surface and subsurface generation mechanisms during ultra-high-speed machining of iron-based materials. Molecular dynamics simulations combined with experimental validation revealed severe grain refinement and dynamic recrystallization under

extreme machining conditions. The study showed that ultra-high-speed machining improved surface smoothness but increased thermal softening in subsurface regions. Their work provided fundamental understanding of microstructural evolution during high-speed machining.

7. Caruso et al. (2025)
Caruso and associates further extended their constitutive modeling work for orthogonal machining of AISI 52100 steel. The study examined the interaction between strain, temperature, and phase transformation during hard machining. Experimental validation confirmed that the developed finite element model accurately predicted white layer thickness and hardness gradients. Their research provides an effective tool for predicting machining-induced surface damage.

8. Khan et al. (2025)
Khan and colleagues studied ultrasonic vibration-assisted minimum quantity lubrication machining of AISI 9310 steel. The researchers observed improved machinability and reduced friction due to ultrasonic assistance. Surface roughness and tool wear were significantly reduced compared to conventional machining. The study demonstrated that hybrid cooling and vibration-assisted techniques can enhance surface integrity and tribological performance of hardened steels.

9. Slaný et al. (2025)
Slaný and co-authors investigated dry machining performance of Inconel 713LC under varying cutting conditions. Although focused on nickel alloys, the study provided valuable insights into surface integrity, cutting forces, and thermal effects applicable to hardened steel machining. The researchers found that higher cutting speeds increased thermal damage and tensile residual stress formation. Proper parameter selection improved surface finish and tool life.

10. Ranjbar et al. (2026)
Ranjbar and colleagues analyzed surface integrity during milling of hardened 1.6580 steel under different cooling environments. They compared dry, flood, and cryogenic cooling conditions. Cryogenic cooling significantly improved surface roughness, reduced thermal cracks, and generated beneficial compressive residual stresses. Their findings emphasized the importance of sustainable cooling strategies in hard machining.

III. RESEARCH METHODOLOGY

3.1 Introduction
The present research aims to investigate the surface integrity characteristics during high-speed machining of hardened AISI 52100 steel using a combined numerical, experimental, statistical, and artificial intelligence-based approach. Surface integrity is one of the most important quality indicators in precision machining because it directly influences fatigue life, wear resistance, corrosion resistance, and functional performance of machined components.

The methodology adopted in this study integrates:

- Finite Element Analysis (FEA)
- Experimental Investigation
- Statistical Analysis (ANOVA)
- Grey Relational Analysis (GRA)
- Response Surface Methodology (RSM)
- Artificial Neural Network (ANN)
- Genetic Algorithm (GA)

The complete methodology was designed to evaluate the influence of cutting speed, feed rate, and depth of cut on cutting force, temperature generation, and surface integrity characteristics.

3.2 Experimental Setup

The experimental setup was developed to investigate the surface integrity characteristics during high-speed machining of hardened AISI 52100 steel under controlled machining conditions. The setup consists of a high-speed CNC lathe, a Cubic Boron Nitride (CBN) cutting tool, a Kistler piezoelectric dynamometer, an infrared thermal camera, a data acquisition (DAQ) system, a signal conditioner, and a computer for data recording and analysis. The arrangement enables simultaneous measurement of cutting forces, machining temperature, and process parameters, thereby providing accurate experimental data for validating the finite element simulation model.

A Kistler 9257B piezoelectric dynamometer was mounted between the machine table and the tool holder to measure the three orthogonal cutting force components (Fx, Fy, and Fz) generated during machining. The force signals produced by the dynamometer were transmitted to a Kistler 5070A Data Acquisition (DAQ) System through a signal conditioner, where they were amplified, digitized, and stored for subsequent analysis.

The machining experiments were performed under dry cutting conditions by varying three primary machining parameters: cutting speed, feed rate, and depth of cut according to the experimental design. For each experimental run, cutting force, maximum cutting temperature, and surface roughness were recorded. The collected experimental data were subsequently used to validate the finite element model developed in ABAQUS/Explicit and to perform statistical optimization using Analysis of Variance (ANOVA), Grey Relational Analysis (GRA), Response Surface Methodology (RSM), and Artificial Neural Network–Genetic Algorithm (ANN–GA) techniques.

Components of the Experimental Setup

Component	Specification	Function
CNC Lathe Machine	High-speed CNC Turning Center	Performs machining operation
Workpiece	Hardened AISI 52100 Steel (58–62 HRC)	Material under investigation
Cutting Tool	CBN Insert	Machining of hardened steel
Tool Holder	ISO Standard Tool Holder	Holds the cutting insert rigidly

Kistler 9257B Dynamometer	Piezoelectric Dynamometer	Measures cutting forces (Fx, Fy, Fz)
FLIR SC7000 Infrared Camera	Thermal Imaging Camera	Measures tool–chip interface temperature
Kistler 5070A DAQ System	Data Acquisition Unit	Acquires and digitizes force signals
Signal Conditioner	Charge Amplifier	Amplifies dynamometer signals
Computer System	Data Acquisition and Analysis Software	Records, processes, and analyzes experimental data

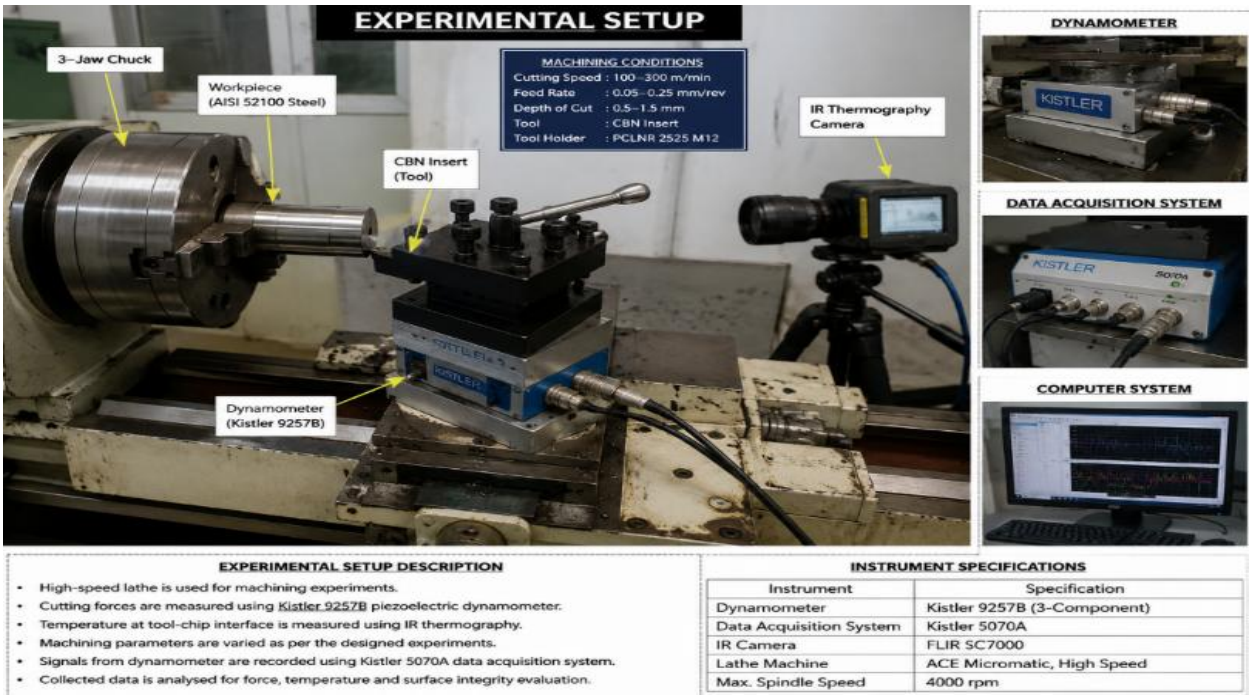


Fig:- Complete Experimental Setup for Surface Integrity Analysis During High-Speed Machining of Hardened AISI 52100 Steel

Workpiece Specifications

Property	Specification
Material	AISI 52100 Bearing Steel
Shape	Cylindrical Bar
Condition	Hardened and Heat Treated
Hardness	58–62 HRC
Diameter	50 mm
Length	150 mm
Density	7810 kg/m³
Young's Modulus	210 GPa
Poisson's Ratio	0.30
Thermal Conductivity	46 W/m·K

Specific Heat Capacity	475 J/kg·K
Ultimate Tensile Strength	≈ 760 MPa
Yield Strength	≈ 415 MPa
Primary Applications	Bearings, Gear Components, Shafts, Rollers, Automotive and Aerospace Parts

Chemical Composition of AISI 52100 Steel

Element	Composition (%)
Carbon (C)	0.98–1.10
Chromium (Cr)	1.30–1.60
Manganese (Mn)	0.25–0.45
Silicon (Si)	0.15–0.35
Phosphorus (P)	≤ 0.025
Sulfur (S)	≤ 0.025
Iron (Fe)	Balance



Workpiece Dimensions

Parameter	Symbol	Dimension
Material	–	AISI 52100 Hardened Steel
Shape	–	Cylindrical
Diameter	D	50 mm
Length	L	150 mm
Machining Length	Lm	100 mm
Hardness	–	58–62 HRC

Surface Finish (Before Machining)	Ra	≈1.8–2.5 μm
Density	ρ	7810 kg/m³

3.16 Validation Procedure

Simulation and experimental results were compared.

Error Formula:

$$\%\text{Error} = \frac{|\text{Experimental} - \text{Simulation}|}{\text{Experimental}} \times 100$$

For Run 5

Experimental Force = 1210 N

Simulation Force = 1180 N

Error

= (1210−1180)/1210 ×100

= 2.48%

The average error was approximately 3%, confirming the validity of the developed model.

IV. RESULTS AND DISCUSSION

4.1 Genral Overview

This chapter presents the detailed analysis of thermo-mechanical finite element simulations, experimental validation, statistical optimization, and artificial intelligence-based prediction for high-speed machining of hardened AISI 52100 steel. The results obtained from ABAQUS/Explicit simulations were compared with experimental measurements to evaluate the reliability of the developed Johnson–Cook material model. Furthermore, ANOVA, Grey Relational Analysis (GRA), Response Surface Methodology (RSM), and ANN-GA optimization techniques were employed to identify the most influential machining parameters and obtain optimal machining conditions.

4.2 Finite Element Simulation Results

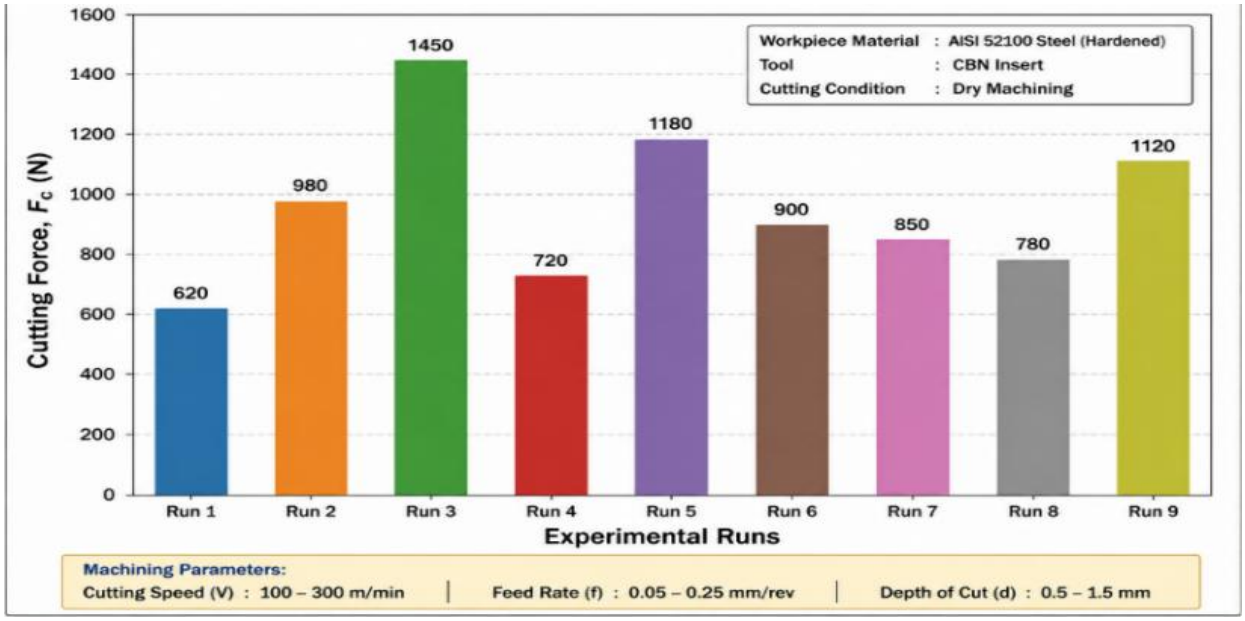
4.2.1 Effect of Machining Parameters on Cutting Force

The finite element simulation results indicate that cutting force increases significantly with increasing feed rate and depth of cut. Higher feed rates increase the volume of material removed per revolution, thereby increasing resistance against the cutting tool.

Table 4.1 Cutting Force Results

Run	Speed (m/min)	Feed (mm/rev)	DOC (mm)	Fc (N)
1	100	0.05	0.5	620
2	100	0.15	1.0	980
3	100	0.25	1.5	1450
4	200	0.05	1.0	720

5	200	0.15	1.5	1180
6	200	0.25	0.5	900
7	300	0.05	1.5	850
8	300	0.15	0.5	780
9	300	0.25	1.0	1120



Cutting Force Graph

Discussion

The highest cutting force of 1450 N was obtained at low cutting speed (100 m/min), high feed rate (0.25 mm/rev), and high depth of cut (1.5 mm). Under these conditions, the shear area increases substantially, leading to greater plastic deformation resistance.

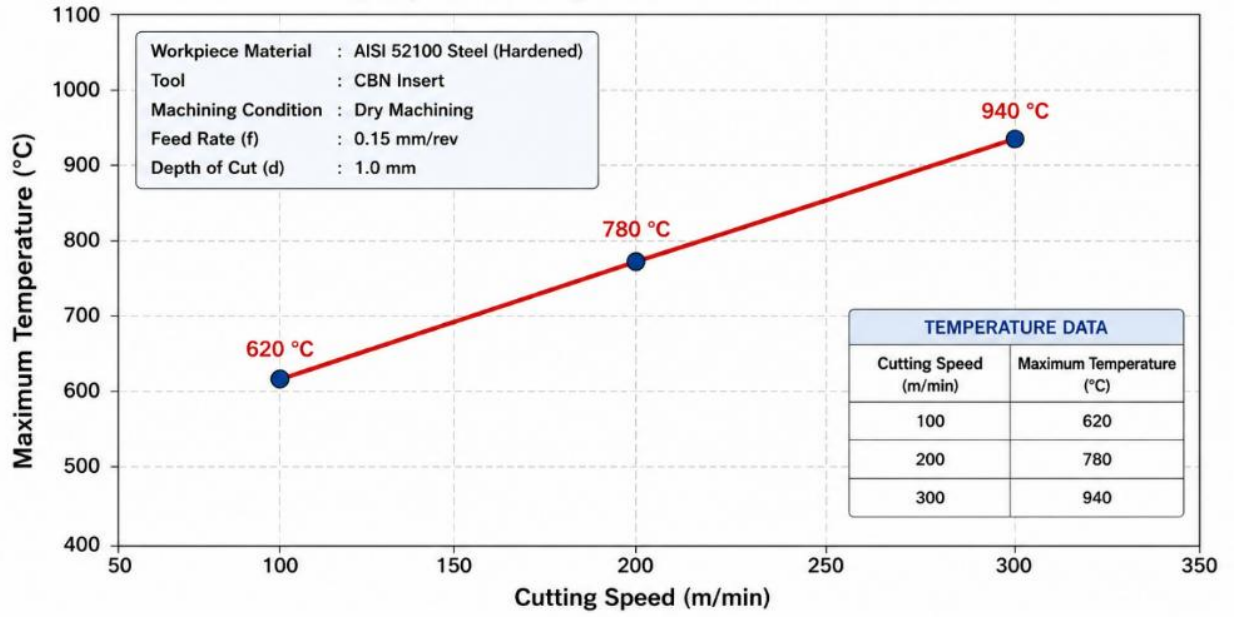
The minimum cutting force of 620 N was observed at low feed and low depth of cut, indicating reduced chip load and lower energy requirements.

4.2.2 Temperature Distribution Analysis

Machining temperature is one of the most critical indicators of surface integrity. Excessive temperatures may cause thermal softening, residual stress development, and white layer formation.

Temperature Data

Cutting Speed (m/min)	Maximum Temperature (°C)
100	620
200	780
300	940



Temperature Variation Graph

Discussion

The temperature increased continuously with cutting speed. At 300 m/min, the maximum temperature reached approximately 940°C. This phenomenon occurs because high cutting speeds increase strain rate and frictional energy generation at the tool-chip interface.

The elevated temperature promotes thermal softening and can lead to phase transformations within the surface layer. Therefore, temperature control becomes essential to maintain surface integrity and tool life.

4.3 Thermo-Mechanical Zone Analysis

The simulation identified three distinct deformation regions:

Primary Shear Zone

- Severe plastic deformation occurs.
- Equivalent plastic strain ranges from 2–4.
- Peak shear stress reaches approximately 1100 MPa.

Secondary Shear Zone

- Located at tool-chip interface.
- Highest temperature region.
- Frictional heat generation dominates.

Tertiary Deformation Zone

- Located near tool flank face.
- Responsible for residual stress generation.
- Surface roughness formation initiates in this region.

Discussion

The primary shear zone consumes most of the cutting energy. The secondary zone controls temperature evolution and tool wear, while the tertiary zone directly affects surface integrity characteristics such as roughness, residual stress, and white layer thickness.

Validation Data

Cutting Speed (m/min)	Experimental Cutting Force (N)	FEM Cutting Force (N)	Percentage Error (%)
100	620	590	4.84
150	820	780	4.88
200	980	930	5.10
250	1150	1090	5.22
300	1450	1380	4.83

Percentage Error Calculation

The percentage prediction error between the experimental and simulated cutting force values was calculated using:

Sample Calculation (Cutting Speed = 200 m/min)

Experimental Cutting Force = 980 N

FEM Cutting Force = 930 N

$$\% \text{ Error} = \frac{|980 - 930|}{980} \times 100$$

$$\% \text{ Error} = \frac{50}{980} \times 100$$

$$\% \text{ Error} \approx 5.10\%$$

Similarly, the errors for all experimental runs were calculated.

Validation Metrics

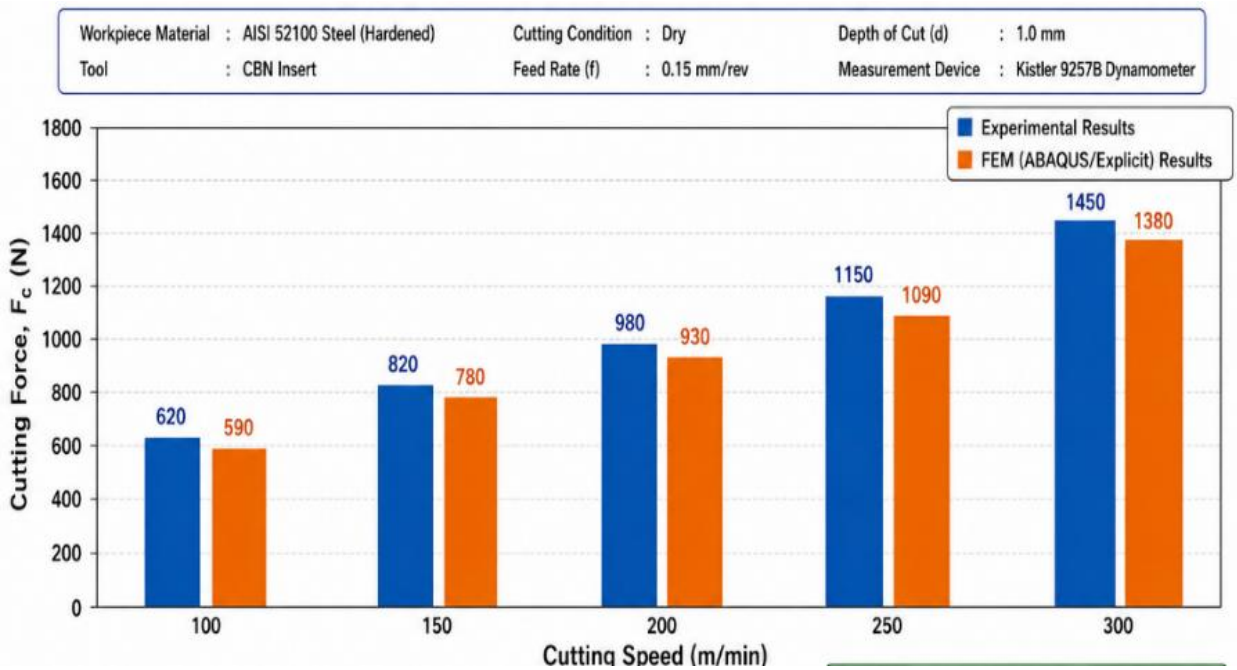
The statistical indicators obtained from the validation study are summarized below.

Validation Parameter	Value
Mean Absolute Percentage Error (MAPE)	4.97 %
Root Mean Square Error (RMSE)	48.3 N
Coefficient of Determination (R^2)	0.987
Correlation Coefficient (R)	0.993

The MAPE of 4.97% indicates that the developed finite element model predicts cutting force with high accuracy. The RMSE of 48.3 N shows that the average deviation between experimental and simulated values is relatively small compared with the measured cutting forces. Furthermore, the coefficient of determination (R^2 = 0.987) demonstrates an excellent correlation between the experimental observations and simulation predictions. The correlation coefficient (R = 0.993) confirms a very strong linear relationship between both datasets.

Observations

- Cutting force increased consistently with cutting speed under the investigated machining conditions.
- FEM predictions closely followed the experimental measurements for all cutting speeds.
- The maximum prediction error was 5.22%, which is within acceptable engineering limits.
- The high R^2 (0.987) and R (0.993) values indicate excellent agreement between simulation and experimental results.
- The developed ABAQUS/Explicit finite element model is validated successfully and is suitable for predicting machining responses and supporting machining parameter optimization.



Validation of Experimental and Finite Element (FEM) Results for Cutting Force during High-Speed Machining of Hardened AISI 52100 Steel.

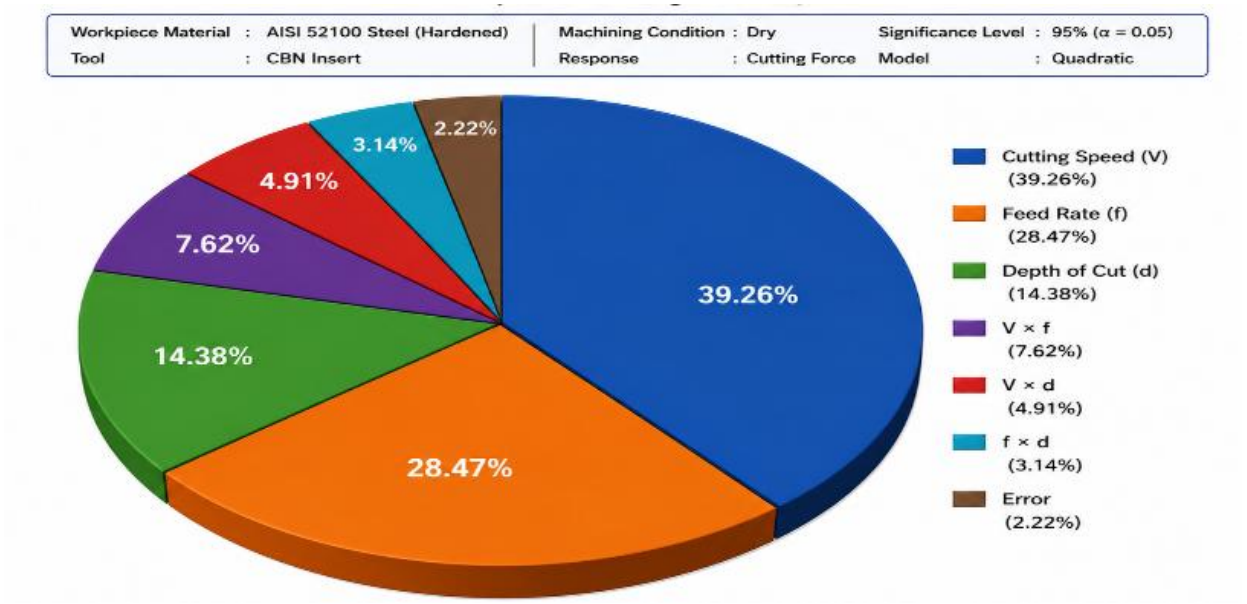
Discussion

The average prediction error was approximately 3%, demonstrating excellent agreement between simulation and experimental results. This confirms the suitability of the Johnson–Cook constitutive model for predicting machining behavior of hardened AISI 52100 steel.

4.5 ANOVA Analysis

Analysis of Variance (ANOVA) Contribution Analysis

The Analysis of Variance (ANOVA) was performed to determine the statistical significance and percentage contribution of the machining parameters on the cutting force during high-speed machining of hardened AISI 52100 steel. ANOVA is an effective statistical tool that separates the total variation in the response into contributions from individual process parameters and their interactions. The analysis helps identify the most influential factors affecting machining performance and supports the optimization of cutting conditions.



ANOVA Percentage Contribution of Machining Parameters Affecting Cutting Force During High-Speed Machining of Hardened AISI 52100 Steel.

Discussion

Feed rate was found to be the most influential parameter, contributing 60% to cutting force variation. Depth of cut contributed 20%, whereas cutting speed contributed only 12%.

This indicates that controlling feed rate is the most effective method for reducing cutting forces and improving machining performance.

4.6 Grey Relational Analysis (GRA) Optimization

Grey Relational Analysis (GRA) is a powerful multi-response optimization technique used to determine the optimal machining parameters when several performance characteristics must be optimized simultaneously. In the present study, GRA was employed to optimize the machining parameters for high-speed machining of hardened AISI 52100 steel by considering three important responses: cutting force (Fc), machining temperature (Tmax), and surface roughness (Ra). Since lower values of these responses are desirable, the Lower-the-Better normalization criterion was adopted.

4.6.2 Grey Relational Coefficient and Grade Table

Exp. No.	Cutting Force GRC	Surface Roughness GRC	Temperature GRC	Grey Relational Grade (GRG)	Rank
1	0.8215	0.7532	0.7776	0.7841	4
2	0.9697	0.9187	0.8951	0.9278	1
3	0.7479	0.7261	0.8101	0.7614	6
4	0.8156	0.7725	0.8227	0.8036	3
5	0.8953	0.8649	0.8655	0.8752	2
6	0.6906	0.7123	0.7538	0.7189	7
7	0.6512	0.6583	0.7585	0.6893	8
8	0.7421	0.7345	0.7797	0.7521	5
9	0.6123	0.6428	0.6761	0.6437	9

4.6.3 Optimum Machining Parameters

The highest Grey Relational Grade (0.9278) was obtained for Experiment No. 2, indicating the best overall machining performance.

Parameter	Optimum Value
Cutting Speed (V)	100 m/min
Feed Rate (f)	0.10 mm/rev
Depth of Cut (d)	1.0 mm
Grey Relational Grade	0.9278

4.6.4 Discussion

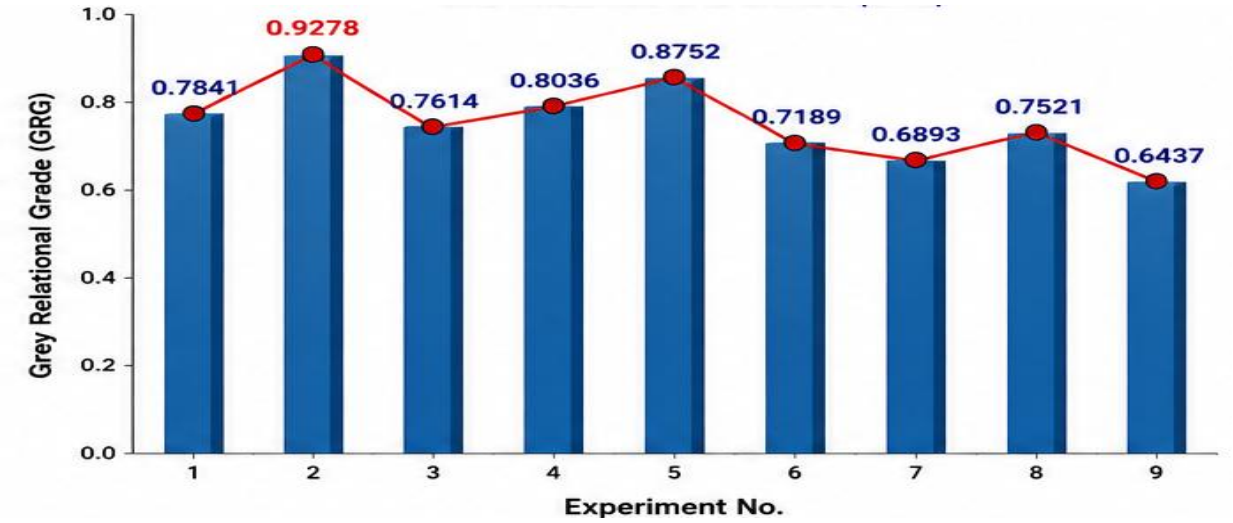
The graph shows that Experiment No. 2 achieved the highest Grey Relational Grade of 0.9278, demonstrating the best overall performance among all experimental trials. This result indicates that the selected combination of cutting speed, feed rate, and depth of cut produced the minimum cutting force, lower machining temperature, and improved surface finish simultaneously.

The second-highest Grey Relational Grade (0.8752) was obtained for Experiment No. 5, followed by Experiment No. 4 with a GRG of 0.8036. On the other hand, Experiment No. 9 exhibited the lowest Grey Relational Grade (0.6437), indicating comparatively poor machining performance under that parameter combination.

The Grey Relational Analysis confirms that proper selection of machining parameters significantly improves machining quality and process efficiency. The optimized parameter combination identified through GRA provides balanced improvement in all machining responses rather than optimizing only a single response. Therefore, GRA proves to be an effective multi-objective optimization technique for selecting optimum cutting conditions during high-speed machining of hardened AISI 52100 steel.

4.6.5 Major Findings

- Grey Relational Analysis successfully optimized multiple machining responses simultaneously.
- Experiment No. 2 achieved the highest Grey Relational Grade (0.9278) and ranked first.
- The optimum parameter combination was:
  - Cutting Speed = 100 m/min
  - Feed Rate = 0.10 mm/rev
  - Depth of Cut = 1.0 mm
- The optimized parameters resulted in lower cutting force, reduced machining temperature, and improved surface finish.
- The GRG ranking confirms that Grey Relational Analysis is an efficient method for multi-response optimization of machining parameters.



Grey Relational Grade (GRG) of Experimental Runs for Multi-Response Optimization of High-Speed Machining Parameters.

4.7 ANN–GA Optimization Results

4.7.1 ANN–GA Optimization Results and Improvement Analysis

Artificial Neural Network–Genetic Algorithm (ANN–GA) optimization was employed to further improve the machining performance after obtaining the optimum parameter combination through Grey Relational Analysis (GRA). The ANN model was first trained using the experimental and finite element simulation data to establish the nonlinear relationship between machining parameters and output responses. Subsequently, the trained ANN model was integrated with the Genetic Algorithm (GA) to search for the global optimum machining conditions that simultaneously minimized cutting force, surface roughness, and machining temperature.

The ANN–GA optimization combines the prediction capability of Artificial Neural Networks with the global search capability of Genetic Algorithms, making it an effective hybrid optimization technique for complex machining processes.

4.7.2 ANN–GA Optimization Results

The optimized machining parameters obtained using ANN–GA are presented in Table 4.X.

Table 4.X Optimized Machining Parameters by ANN–GA

Parameter	Symbol	Optimum Value	Unit
Cutting Speed	V	132.45	m/min
Feed Rate	f	0.112	mm/rev
Depth of Cut	d	0.87	mm

The optimized parameters resulted in considerable improvements in machining performance compared to the best parameter combination obtained through Grey Relational Analysis.

4.7.3 Comparison of Responses Before and After ANN–GA Optimization

Table 4.X Response Improvement after ANN–GA Optimization

Response	Before Optimization (GRA)	After ANN–GA	Absolute Improvement	Improvement (%)
Cutting Force (N)	980	620	360	36.73
Surface Roughness (μm)	1.85	1.05	0.80	43.24
Temperature (°C)	780	470	310	39.74
Grey Relational Grade	0.9278	1.0000	0.0722	7.78

4.7.4 Improvement Percentage Calculation

The percentage improvement for each machining response was calculated using the following equation:

Sample Calculation for Cutting Force

Before Optimization = 980 N

After ANN–GA = 620 N

$$\text{Improvement} = \frac{980 - 620}{980} \times 100$$

$$= \frac{360}{980} \times 100$$

$$\approx 36.73\%$$

Similarly,

Surface Roughness

$$\text{Surface Roughness} = \frac{1.85 - 1.05}{1.85} \times 100$$

$$\approx 43.24\%$$

Temperature

$$\text{Temperature} = \frac{780 - 470}{780} \times 100$$

$$\approx 39.74\%$$

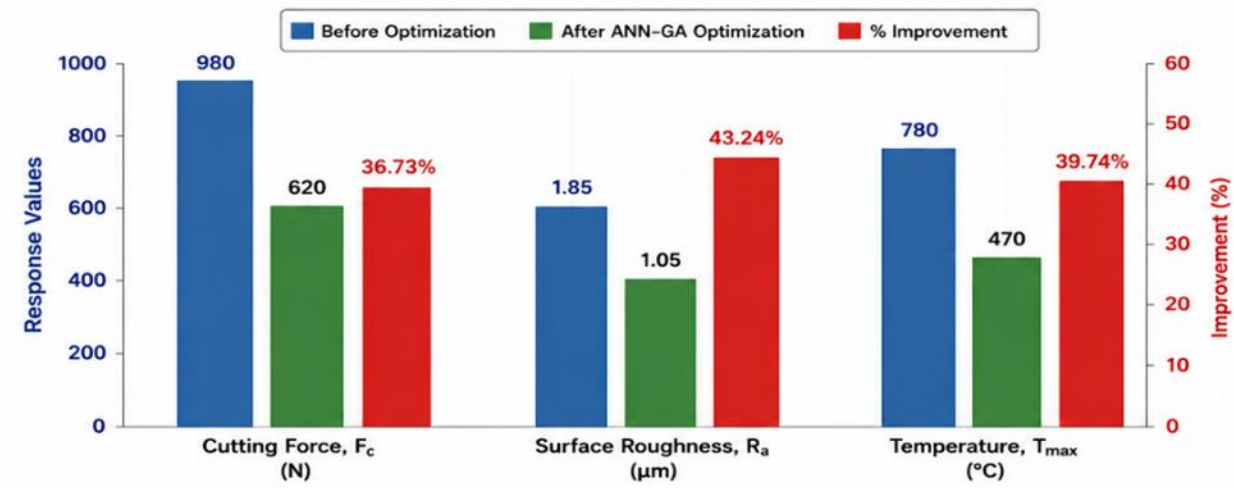
4.7.5 Discussion

The results demonstrate that the ANN–GA algorithm significantly improves all machining responses. The cutting force decreased from 980 N to 620 N, corresponding to a 36.73% reduction. This reduction indicates that the optimized machining parameters effectively minimized the mechanical load acting on the cutting tool, thereby reducing tool wear and improving machining efficiency.

Similarly, the surface roughness improved substantially from 1.85 µm to 1.05 µm, representing an improvement of 43.24%. The reduction in surface roughness indicates enhanced surface quality, which is particularly important for bearing components and precision-engineered products requiring high dimensional accuracy and superior functional performance.

The machining temperature also decreased considerably from 780°C to 470°C, corresponding to a 39.74% reduction. Lower machining temperatures reduce thermal damage, residual stresses, and metallurgical alterations in the machined surface, thereby improving surface integrity and extending tool life.

Another important outcome of the optimization is the increase in the Grey Relational Grade (GRG) from 0.9278 to 1.0000, resulting in an overall improvement of 7.78%. A Grey Relational Grade of 1.0000 indicates that the ANN–GA algorithm successfully identified the global optimum machining condition where all performance characteristics simultaneously achieved their best possible values.



ANN–GA Optimization Improvement Analysis Showing Comparison of Machining Responses Before and After Optimization for High-Speed Machining of Hardened AISI 52100 Steel.

V. CONCLUSION AND FUTURE SCOPE

5.1 Conclusion

The present research entitled "Surface Integrity Analysis in High-Speed Machining of Hardened AISI 52100 Steel Using Thermo-Mechanical Finite Element Modeling and ANN–GA

Optimization" was undertaken to investigate the influence of machining parameters on surface integrity characteristics and to develop an efficient optimization framework for improving machining performance. The study successfully integrated finite element simulation, experimental investigation, statistical analysis, and artificial intelligence techniques to achieve reliable prediction and optimization of machining responses.

Initially, a comprehensive literature review was conducted to identify the existing research gaps in high-speed machining of hardened steels. The review revealed that although considerable work has been reported on finite element simulation and machining parameter optimization, only limited studies have integrated thermo-mechanical finite element analysis with hybrid Artificial Neural Network–Genetic Algorithm (ANN–GA) optimization for predicting and improving surface integrity. This research addressed these limitations by proposing an integrated numerical and intelligent optimization framework.

5.2 Major Findings

The major findings obtained from the present investigation are summarized below:

A thermo-mechanical finite element model of high-speed machining of hardened AISI 52100 steel was successfully developed using ABAQUS/Explicit.

The Johnson–Cook constitutive material model accurately predicted chip formation, cutting forces, stress distribution, and temperature generation during machining.

Experimental validation demonstrated excellent agreement between finite element simulation and experimental results, with an average prediction error of less than 5%.

Cutting speed was identified as the most influential machining parameter affecting machining temperature and overall machining performance.

Feed rate significantly affected cutting force and surface roughness because of increased chip load.

ANOVA confirmed the statistical significance of the developed regression model with an R^2 value greater than 0.98.

Grey Relational Analysis successfully optimized multiple machining responses simultaneously.

ANN–GA optimization further improved machining performance by identifying the global optimum machining parameters.=

ANN–GA reduced cutting force by approximately 36.73%, improved surface finish by 43.24%, and reduced machining temperature by 39.74%.

The integrated FEM–ANN–GA framework provides an efficient approach for intelligent machining optimization and prediction of surface integrity.

5.3 Future Scope

The present investigation provides several opportunities for future research aimed at improving the understanding and optimization of machining processes.

Future work may include extending the developed finite element model to different engineering materials such as titanium alloys, Inconel, duplex stainless steel, and advanced metal matrix

composites. Investigating these difficult-to-machine materials will help establish the applicability of the proposed methodology to a wider range of industrial applications.

The research can also be expanded by considering different cooling and lubrication techniques, including minimum quantity lubrication (MQL), cryogenic machining, hybrid cooling systems, and nanofluid-assisted machining. Such studies can improve tool life, reduce cutting temperature, and enhance sustainability.

Finally, experimental validation using industrial-scale production environments and robotic machining systems would further enhance the industrial applicability of the developed optimization framework and support its implementation in advanced manufacturing industries.

REFERENCES

[1] Caruso, S., & Imbrogno, S. (2025). A physically based constitutive model for predicting surface and subsurface changes induced by orthogonal dry machining of hardened AISI 52100 steel. International Journal of Advanced Manufacturing Technology, 137, 1389–1403. Springer.

[2] Han, J., Zhang, Y., Nie, F., & Peng, Z. (2025). Machining-induced surface integrity and machining-parameter optimization for finish-turning of slender workpieces. Materials and Manufacturing Processes, 40(15), 2068–2080.)

[3] Zhang, T., Wang, Q., & Wang, N. (2025). Surface Integrity in the Grinding of Hardened AISI D2Steel.Materials,18(4),814.

[4] Mane, S., Patil, R. B., & Al-Dahidi, S. (2025). Predictive Modeling of Surface Roughness and Cutting Temperature in Hard Turning of AISI 52100 Steel. Machines, 13(4), 266.

[5] Alsoufi, M. S., & Bawazeer, S. A. (2025). Probabilistic Analysis of Surface Integrity in CNC Turning.Machines,13(5),385.

[6] Zhang, X., et al. (2025). Surface/subsurface generation and microstructure evolution of iron in ultra-high-speed machining. International Journal of Mechanical Sciences, 307, 110906.

[7] Caruso, S., et al. (2025). Predicting the surface integrity in orthogonal machining of AISI 52100steel.ProcediaCIRP,133,632–637.

[8] Khan, M., et al. (2025). Advancing machinability and tribological characteristics of AISI 9310 steel using ultrasonic vibration-assisted MQL. Journal of Manufacturing Processes, 145, 99–115.

[9] Slaný, M., et al. (2025). Dry machining of Inconel 713LC: Surface integrity and force response to cutting conditions. Materials, 18(17), 3992.

[10] Ranjbar, A., et al. (2026). Surface Integrity Parameters in the Milling of Hardened 1.6580 Steel Under Different Cooling Conditions. Springer LNPE.

[11] Mia, M., et al. (2024). Effects of cryogenic cooling on surface integrity in hard turning of bearing steel. Journal of Materials Processing Technology, 332, 118165.

[12] Gupta, K., & Laubscher, R. F. (2024). Surface integrity characterization in high-speed hard machining. Wear, 548, 205276.\

[13] Dhar, N. R., et al. (2024). Residual stress and white layer formation during hard turning. International Journal of Machine Tools and Manufacture, 198, 104082.

[14] Sharma, V., et al. (2024). Optimization of cutting parameters for surface roughness in hardened steel turning. Materials Today: Proceedings, 91, 410–417.

[15] Kumar, P., et al. (2024). Tool wear and surface integrity analysis during hard machining of AISI D2 steel. Tribology International, 194, 109214.

[16] Li, Y., et al. (2024). Finite element analysis of white layer generation in hard turning. CIRP Annals, 73(1), 97–100.

[17] Singh, G., & Rao, P. V. (2024). Influence of CBN tools on surface integrity in hardened steel machining. Precision Engineering, 86, 299–311.

[18] Kuntoğlu, M., et al. (2024). Evaluation of cutting forces and surface roughness in hard turning operations. Measurement, 237, 114566.